

Wicking within forests of micropillars

C. ISHINO^{1,2}, M. REYSSAT¹, E. REYSSAT¹, K. OKUMURA² and D. QUÉRÉ¹

¹ *Physique et Mécanique des Milieux Hétérogènes, UMR 7636 du CNRS, ESPCI - 10 rue Vauquelin, 75005 Paris, France*

² *Department of Physics, Graduate School of Humanities and Sciences, Ochanomizu University Tokyo 112-8610, Japan*

received 18 May 2007; accepted in final form 19 July 2007

published online 8 August 2007

PACS 68.08.Bc – Wetting

PACS 68.35.Md – Surface thermodynamics, surface energies

PACS 85.40.Hp – Lithography, masks and pattern transfer

Abstract – We describe how a wetting liquid brought into contact with a forest of micropillars impregnates this forest. Both the driving and the viscous forces depend on the parameters of the texture (radius b and height h of the pillars, pitch p of the network) and it is found that two different limits characterize the dynamics of wicking. For small posts ($h < p$), the film progresses all the faster since the posts are high, allowing a simple control of this dynamics. For tall pillars ($h > p$), the speed of impregnation becomes independent of the pillar height, and becomes mainly fixed by the radius of the posts.

Copyright © EPLA, 2007

Wicking is one of the most important phenomena in surface science, both from the practical and historical points of view: the classical experiments on capillary rise by Hauksbee, (Brook) Taylor, and Jurin around 1700 led Young and Laplace to establish the basic principles of this science in 1805. As we all know today, a liquid will penetrate a tube of constant diameter provided that the surface energy of the wet tube is lower than that of the dry one. Denoting γ_{SL} and γ_{SV} as the solid/liquid and solid/vapour surface energies, this criterion is written $\gamma_{SL} < \gamma_{SV}$. The quantity $\gamma_{SV} - \gamma_{SL}$ can thus be viewed as the force (per unit length) which draws the meniscus inside the tube. Introducing the contact angle θ of the liquid on the solid, we deduce from Young's relation ($\gamma_{SV} - \gamma_{SL} = \gamma \cos \theta$, with γ the liquid/vapour surface tension) that the criterion of wicking can also be expressed as $\theta < 90^\circ$.

If the liquid completely wets the tube walls, the wicking process can be viewed as slightly different. Then, a film of molecular thickness propagates along the walls of the tube [1]. The advancing motion of the macroscopic meniscus can then be understood as arising from the suppression of the liquid/vapour interface present along the tube, owing to this precursor film. Hence, the driving force (per unit length) in this case is just γ . We deduce from this consideration the final height of the rise (for a vertical tube), for which this force is balanced by the weight of the liquid column. It also gives access to the dynamics of the liquid penetration: neglecting gravity

(which corresponds to horizontal tubes, or to scales much smaller than the final height), we can balance the constant driving force (of the order of γb , where b is the tube radius) with the viscous friction (which scales as $\eta V z$, denoting V as the velocity of the meniscus, z as its position, and η as the liquid viscosity). We thus find the famous Washburn law, which stipulates that the position of the meniscus increases as the square root of time: $z \sim (Dt)^{1/2}$, with D a dynamic coefficient depending on both the nature of the liquid and the tube radius ($D \sim \gamma b / \eta$) [2]. This law remarkably resists the complexity of “real” systems: it is found that such dynamics are observed both for liquid spreading on rough solids [3–5], and for wicking in most porous media, such as paper, fabrics and sand.

Here we discuss the propagation of liquids along solids decorated with a forest of micropillars. These pillars could be silicon posts, carbon nanotubes, or even simple hairs [6]. These surfaces recently attracted a lot of attention, in particular because of their remarkable wetting properties. If hydrophobic and tall enough, the small-diameter posts literally “repel” water: if the density of pillars is low (area fraction typically between 1 and 10 percent), the liquid mainly sits on air, which provides spectacular superhydrophobic properties [7]. Here we consider the opposite limit where the liquid wets the material, so that it is likely to propagate inside the forest as if it were some (nearly two-dimensional) porous medium [5,8]. This kind of device can be used for introducing obstacles in a flow, in the field

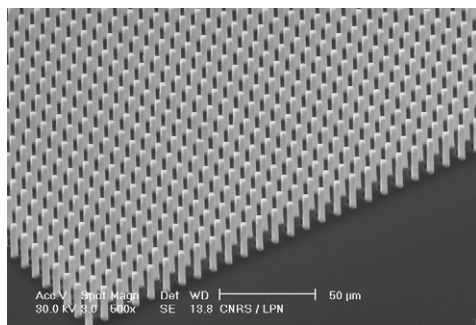


Fig. 1: Silicon surface decorated with a forest of micropillars of radius $b = 1.3 \mu\text{m}$ and height $h = 26 \mu\text{m}$ regularly displayed on a square pattern of pitch $p = 10 \mu\text{m}$. The bar indicates $50 \mu\text{m}$.

of polymer chromatography or DNA electrophoresis, for example [9]. We shall characterize the force driving the motion and show how the dynamics of the wicking can be selected by the texture properties. As we shall see, using such textures is a very convenient way to speed up the spreading of a liquid at a large scale, and to tune the thickness of the spreading film.

We present in fig. 1 a typical sample on which experiments were done. Using techniques from microelectronics (photolithography, deep reactive ion etching), we performed selective etching on a silicon wafer, so that the whole material is made of silicon. Our fabrication techniques allowed us to choose independently the values of the pillar radius b , height h and pitch p . In these experiments, b and p are fixed (about 1 and 10 micrometers, respectively), but h is varied between 1 and 26 micrometers. This gives access to the regimes $h < p$ (short pillars) and $h > p$ (tall pillars), which will be found to generate different dynamics of wicking. Note also that the typical sizes of the microstructures guarantee that gravity can be neglected for our centimetric samples, even if displayed vertically.

Our experiments consisted of bringing samples into contact with a bath of silicone oil. A film was observed to rise along the materials, and its progression was monitored with a camera. The position z of the liquid front was extracted from the movies, by taking advantage of the darkening of the textured solid as oil fills its cavities. Plotting z as a function of time t , we found that Washburn's law was always obeyed (except at very short time): z increases linearly with the square root of t , as seen in fig. 2, where we show how the dynamic coefficient D is extracted from the data.

We measured the value of the coefficient D on various samples, and for each of them we tested oils of different viscosities. A series of results such as displayed in fig. 3 was obtained. For each oil, D is observed to increase with the pillar height, before saturating at large heights. For a given substrate, this dynamical coefficient decreases as the oil is more viscous, showing the viscous nature of the friction. This observation can be made more precise by

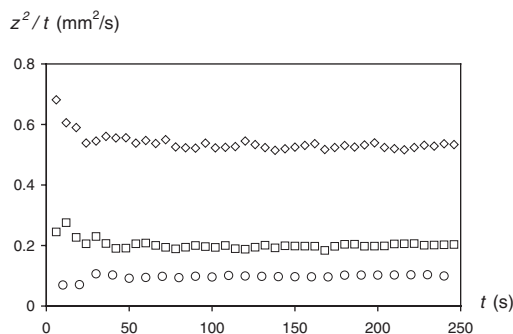


Fig. 2: If a sample decorated with micropillars is brought into contact with a bath of silicone oil, a film progresses inside the forest of pillars. Here we plot the square of the position z of the front divided by the time t as a function of t . The pillars height and pitch are $6 \mu\text{m}$ and $10 \mu\text{m}$. Silicone oils have a surface tension of 20mN/m and a viscosity of 19mPa s (diamonds), 48mPa s (squares) and 97mPa s (circles). We call D the average value of the quantity z^2/t at long time.

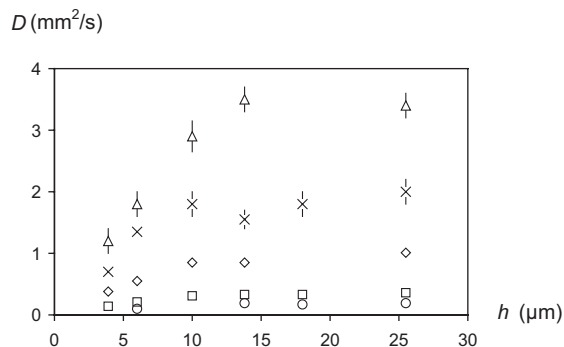


Fig. 3: Dynamical coefficient of wicking D as a function of the height h of the pillars, expressed in micrometers. Oil viscosity is 4.6mPa s (triangles), 9.5mPa s (crosses), 19mPa s (diamonds), 48mPa s (squares) and 97mPa s (circles). The higher the pillars or the less viscous the liquid, the quicker the wicking. However, some saturation of the coefficient D seems to occur for large pillar heights.

plotting D as a function of η , as done for two different pillar heights in fig. 4. For all the samples we studied, it is found that D is inversely proportional to the viscosity, as in Washburn's law. We now discuss the origin of these different behaviours.

If brought into contact with a reservoir of liquid which completely wets the material, a forest of micropillars will suck the liquid (fig. 5). As discussed above for a tube, a molecular layer propagates ahead of the impregnating film, whose driving force thus derives from the energy gained by filling all the cavities between the pillars (since this suppresses all the liquid/vapor interfaces along the pillars). The configuration of minimum energy is obtained if the film thickness matches the post height, as sketched in fig. 5. Thus, if the front of the film advances by a distance dz , the lowering of the liquid/vapour surface energy per

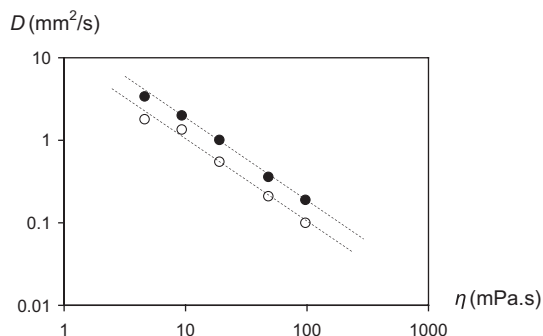


Fig. 4: Dynamical coefficient D as a function of the oil viscosity (between 4.6 and 97 mPa.s). Wicking is observed on a sample decorated with pillars of radius $b = 1.3 \pm 0.2 \mu\text{m}$, pitch $p = 10 \mu\text{m}$, and height $h = 6 \mu\text{m}$ (empty symbols) or $h = 26 \mu\text{m}$ (full symbols). The dotted lines have a slope of -1 .

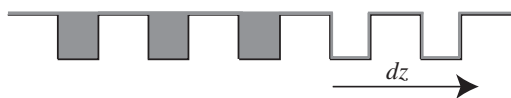


Fig. 5: Progression of a liquid film in a forest of pillars. In the regime of complete wetting, a molecular liquid layer (in grey in the sketch) coats the solid ahead of the impregnating film. As it progresses by dz , the film removes the liquid/vapor interface along the pillars, to which corresponds a lowering of the surface energy by a quantity dE , as analyzed in the text.

unit length of the contact line is $dE = (1 - r)\gamma dz$, where r is the roughness of the substrate (*i.e.*, the ratio between the actual and projected surface areas). Since r is larger than unity, the progression of the film is always favourable ($dE < 0$), in this situation of complete wetting. Hence we deduce the force (per unit width of the film) which provokes wicking. It can be written

$$F = \gamma(r - 1). \quad (1)$$

This force logically only exists if the surface is rough ($r > 1$); the rougher the solid, the larger F . The nature and topography of the texture will thus impact the force driving the liquid inside it. In the case of pillars, we have $r = 1 + 2\pi bh/p^2$, from which we deduce

$$F = 2\pi\gamma \frac{bh}{p^2}. \quad (2)$$

If wetting is only partial, the situation is slightly different. Very generally, the solid will be dry ahead of the film, and the film will be driven by a force $F = -dE/dz = (r - \phi_s)(\gamma_{SV} - \gamma_{SL}) - (1 - \phi_s)\gamma$, denoting ϕ_s as the density of pillars ($\pi b^2/p^2$ in our case). Contrasting with the case of complete wetting, F is not necessarily positive. A film will only progress if $\cos\theta > (1 - \phi_s)/(r - \phi_s)$, that is, if the Young contact angle θ is smaller than a quantity which depends on the characteristics of the surface [5]. Note that the force F derived above reduces to eq. (2) as θ vanishes (which will be the case in our experiments).

We now discuss the nature of the friction associated with the fluid motion. As seen in fig. 4, the friction arises from the liquid viscosity, but several origins are possible. i) The flow generates velocity gradients over a distance h , corresponding to a friction between the moving liquid of thickness h and the bottom solid surface. Integrating over the wet surface area z (written per unit width of the film), we thus find a force F_1 which scales as

$$F_1 \sim \eta \frac{V}{h} z, \quad (3)$$

where $V = dz/dt$ is the velocity of the front.

ii) Liquid friction also takes place against the pillars. Let us first consider an isolated pillar. For a Stokes flow, velocity gradients exist over a distance of the order of b , the pillar radius, and the friction takes place on a surface area bh , from which we deduce a force scaling as ηVh . More exactly, we know that the viscous force acting on a cylinder can be expressed as $\eta Vh/\ln(\lambda/b)$, where λ is a cut-off distance (beyond which we can neglect the influence of the pillar) [10]. If the pillar had an infinite length, λ would be built on a Reynolds number ($\lambda \sim 3.7\eta/\rho V$). More generally, λ is the characteristic distance on which the single pillar perturbs the flow. In our case, where multiple pillars are present, we expect λ to be of the order of p , the pitch of the pillar network. Since we have z/p^2 pillars per unit width of the advancing film, we thus expect a friction F_2 arising from the presence of the pillars scaling as

$$F_2 \sim \frac{\eta Vh z}{p^2 \ln(p/b)}. \quad (4)$$

Of course, both frictions F_1 and F_2 should be present, and oppose the motion. But these two quantities might be quite different. Treating the logarithm as a number (of order one), we find

$$\frac{F_1}{F_2} \sim \frac{p^2}{h^2}. \quad (5)$$

Hence we can distinguish two different cases:

i) For short pillars ($h < p$), the dominant friction arises from the bottom solid surface. Then, balancing the friction F_1 with the driving force F (eq. (2)) yields the law of motion:

$$z^2 = D_1 t \quad (6)$$

with

$$D_1 = \frac{4\pi}{3} \frac{\gamma h^2 b}{\eta p^2} \quad (7)$$

taking into account the numerical coefficient 3 in the Poiseuille law (eq. (3)).

ii) For long pillars ($h > p$), the driving force F is balanced by the friction F_2 . It turns out that Hasimoto calculated explicitly the numerical coefficient for the friction of a liquid progressing in a collection of cylindrical pillars [11,12]. He found, per pillar: $f_2 = 4\pi\eta Vh/(\ln(p/b) - 1.31)$ [12]. Taking into account the number of

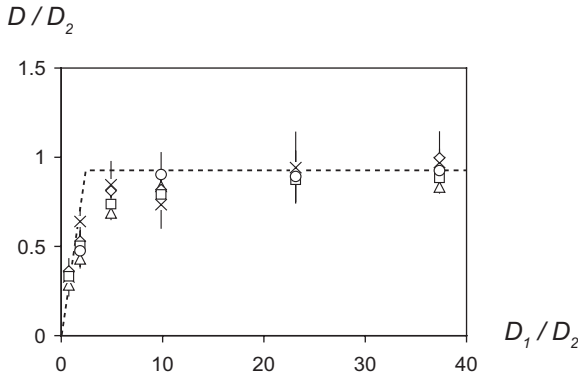


Fig. 6: Experimental dynamical coefficient D of a film moving in a forest of micropillars, as a function of a dimensionless quantity characterizing the topography of the network of pillars. D is normalized by the quantity D_2 given by eq. (9), and of the order of $\gamma b/\eta$. As for the abscissa, D_1 is given by eq. (7), and the calculated quantity D_1/D_2 is just a function of the texture, of the order of h^2/p^2 . The different symbols are for different silicone oils, as in fig. 3.

pillars per unit area, we can finally express the dynamics of the film in this limit. It is written

$$z^2 = D_2 t \quad (8)$$

with

$$D_2 = \frac{\gamma b}{\eta} (\ln(p/b) - 1.31). \quad (9)$$

In both cases, the impregnated length z increases as the square root of time. However, the structure of the dynamical coefficient is quite different according to the pillar height: it first increases rapidly with h (the taller the pillar, the thicker the film, and thus the quicker the movement); then, it becomes independent of the height, because the increase in driving force is exactly compensated by the increase in viscous friction against the pillars. The dynamical coefficient D becomes even nearly independent of the pitch (apart from a logarithmic correction), and turns out to be fixed only by the pillar radius (for a given liquid). Surprisingly, this result is very similar to Washburn's law, replacing the tube radius by the pillar one.

We now compare our experimental data to these models. Increasing the height h of the pillars, we expect the dynamical coefficient D to be successively given by D_1 for short pillars, and by D_2 for tall ones. In order to compare all our results to these expectations, we plot the measured dynamical coefficient D normalized by D_2 as a function of the quantity $D_1/D_2 \sim h^2/p^2$. We first expect a straight line for $D_1/D_2 \ll 1$, till we reach $D_1/D_2 = 1$. Then ($D_1/D_2 \gg 1$), D/D_2 should saturate at a value of order one, whatever the liquid (provided that it wets the material).

This representation is displayed in fig. 6. For each experiment we carefully determined the radius b (using electron microscope photographs such as fig. 1), since

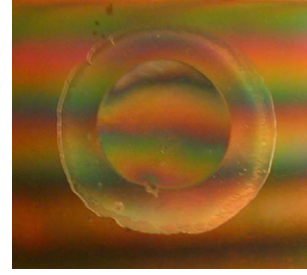


Fig. 7: (Color online) An oil drop (here ethanol) deposited on a microtextured surface in the wicking regime is surrounded by a wetted zone, whose size increases as the square root of time, betraying oil penetration within the pillars. Note that the drop acts as a lens, which deforms the colours arising from the presence of a regular texture.

this parameter enters in both the coefficients D_1 and D_2 . Figure 6 shows a good agreement between observations and our models. First, all the data collapse in a single curve. The dynamical coefficient D first increases as D_1 . In this regime (short pillars, $h < p$), the dynamics of the film can be finely tuned by the pillars height h . This contrasts with the case of larger heights ($h > p$), for which the coefficient D does not depend anymore on h . Then, the coefficient characterizing the liquid progression is close to D_2 (eq. (9)), the value expected from the model, without any adjustable parameter. This result can be regarded as the first confirmation (to the best of our knowledge) of the old calculation by Hasimoto, on the viscous force acting on a liquid flowing in a forest of pillars. This agreement is somehow surprising, if we note that the velocity field in the Hasimoto model is uniform in the direction of the posts, while we expect velocity gradients in this direction, in our case. The threshold between the two regimes is observed around $D_1 = D_2$, that is, $h \sim p$, as expected from the model.

These findings concern the progression of a film from an infinite reservoir, but they also characterize the spreading of a drop deposited on a material textured with assemblies of microposts. Then as observed in fig. 7, a visible spreading zone forms around the drop, showing the progression of a film in the texture (which will affect the spreading dynamics of this drop [13]). Fixing the height of the pillars does not only influence the film dynamics, it also selects its thickness (since surface energy favours a film thickness which matches the pillar height).

It is probably useful to stress how such textures enhance the progression of liquid. A wetting drop which spreads at a large scale is driven by gravity, and the film progression results from a balance between the weight and viscosity. Hence it is found that the radius of the spreading drop increases as $(\rho g \Omega^3 t / \eta)^{1/8}$, where Ω is the drop volume [14]. The time for reaching a given size dramatically depends on this size. We find for example that 10^6 s (about 10 days) are needed to reach 2 cm, for a millimetric drop of a liquid of viscosity as low as that of water. Taking a solid decorated with micropillars in the regime $h > p$,

we find using eq. (8) that the time needed by the film for reaching the same size reduces to 10s —and this dramatic difference would still be larger if considering a bigger wetted spot. This emphasizes how relevant it can be to use such textured materials for speeding up thin film propagation at “large” scales.

We thank Egide and JSPS for its support through a Sakura program, which permitted this collaboration. CI is grateful for the supports from a scholarship from the French Government, and for the Yuasa scholarship of Ochanomizu University. KO thanks MEXT, Japan for KAKENHI. We finally thank Y. CHEN, F. MARTY and A. PÉPIN for helping us to achieve the samples, and Essilor for financial support.

REFERENCES

- [1] DE GENNES P.-G., *Rev. Mod. Phys.*, **57** (1985) 827.
 [2] WASHBURN E. W., *Phys. Rev.*, **17** (1921) 273.
 [3] CAZABAT A. M. and COHEN-STUART M. A., *J. Phys. Chem.*, **90** (1986) 5845.
 [4] APEL-PAZ M. and MARMUR A., *Colloids Surf. A*, **146** (1999) 273.
 [5] BICO J., TORDEUX C. and QUÉRÉ D., *Europhys. Lett.*, **55** (2001) 214.
 [6] WANG Y., SCHMIDT V., SENZ S. and GOSELE U., *Nat. Nanotechnol.*, **1** (2006) 186.
 [7] QUÉRÉ D., *Rep. Prog. Phys.*, **68** (2005) 2495.
 [8] ZHOU J. J., NOCA F. and GHARIB M., *Nanotechnology*, **17** (2006) 4845.
 [9] MINC N., BOKOV P., ZELDOVICH K. B., FUTTERER C., VIOVY J. L. and DORFMAN K. D., *Electrophoresis*, **26** (2005) 362.
 [10] LAMB H., *Hydrodynamics* (Cambridge University Press, Cambridge) 1932.
 [11] HAPPEL J. and BRENNER H., *Low Reynolds Number Hydrodynamics* (Noordhoff International Publishing, Leyden) 1973.
 [12] HASIMOTO H., *J. Fluid Mech.*, **5** (1959) 317.
 [13] MCHALE G., SHIRTCLIFFE N. J., AQIL S., PERRY C. C. and NEWTON M. I., *Phys. Rev. Lett.*, **93** (2004) 036102.
 [14] HUPPERT H. E., *J. Fluid Mech.*, **121** (1982) 43.